

PREDICTION OF CHEMICAL REACTIVITY OF CELLULOSE AND CHITOSAN BASED ON DENSITY FUNCTIONAL THEORY

FERIDE AKMAN

Bingöl University, Vocational School of Technical Sciences, Bingöl 12000, Turkey

✉ *Corresponding author: Feride Akman, chemakman@gmail.com*

Received February 17, 2016

In this work, the molecular structural geometry, the theoretical description of charge distribution, chemical reactivity descriptors, such as electronegativity, chemical hardness, polarizability, electrophilicity index, frontier molecular orbitals (FMOs), molecular electrostatic potential (MEP), electrostatic potential (ESP) and electronic and bonding nature of cellulose and chitosan in dimer structure have been investigated by using the density functional theory in order to gain deeper insights into the nature of these compounds. Chemical reactivity based on the density functional theory (DFT) is useful in identifying the reactive regions of cellulose and chitosan and in analyzing their structures accurately.

Keywords: cellulose, chitosan, DFT, FMOs, MEP, ESP, Mulliken atomic charge

INTRODUCTION

Most polymers are synthetic materials, and their biodegradability and biocompatibility are much more limited than those of natural polymers, such as chitin, chitosan, cellulose and their derivatives. However, natural polymers exhibit a limitation in their processability and reactivity.^{1,2} In this respect, chitosan and its derivatives are recommended as proper functional materials, because these natural polymers have perfect properties, such as non-toxicity, biodegradability, biocompatibility, adsorption properties, *etc.* Recently, increasing attention has been paid to chitosan as a potential polysaccharide resource.³

Cellulose is a homopolymer, while chitosan is the *N*-deacetylated derivative of chitin, and may be fully or partially *N*-deacetylated.⁴ Cellulose is the most abundant naturally occurring biopolymer on the earth and has attracted great interest due to its properties, such as low density, high mechanical strength, biodegradability, low cost, durability, hydrophilicity, non-toxicity, renewability, good film-forming performance, biocompatibility, chemical stability, excellent mechanical properties and the ease of making chemical derivatives.⁵⁻⁹ Cellulose has a broad set of applications in various areas, such as tissue engineering, civil engineering, artificial bones,

dentistry, food packaging, and as contributing additive for polymeric and plastic materials.^{10,11} Recently, cellulose has been also used as separator in lithium-ion battery,¹² water reducing agent in cement,¹³ rheological modifier in drilling fluids,¹⁴ modern wound dressing material,¹⁵ dermatocosmetics for acne treatment¹⁶ and a three-dimensional matrix for bone engineering.¹⁷

Chitosan is also of commercial interest due to its high percentage of nitrogen (6.89%), compared to that of synthetically substituted cellulose (1.25%).¹ Chitosan is produced principally from chitin after alkaline deacetylation and is a biodegradable, non-toxic and biocompatible polymer. Besides, chitosan is a natural inexpensive polysaccharide with a long-chain backbone comprising *N*-acetyl glucosamine.^{4,18} As a hydrophilic polyelectronic polymer, chitosan contains positive charges in acidic condition, and its fluid behaviour can be affected by the number of hydrogen bonds, the molecular configuration and the electrostatic repulsion of neighboring molecules.¹⁹ Most of the literature shows that chitosan offers benefits and positive functions; for this reason, chitosan and its derivatives have become widely used in various industries, in areas such as water engineering, cosmetics, food processing, textile industry, health food, tissue

engineering, agriculture, wound healing, photography and drug delivery systems.^{20,21} Moreover, chitosan has been extensively explored in proton conductors,²² coatings for antimicrobial protection on paper surface,²³ colon-specific drug delivery²⁴ and fertilizer delivery systems.²⁵

The use of chitosan as a bioactive substance to control postharvest fungal disease has also attracted great interest due to public concerns about overuse of chemicals, food safety, fungicide residue, and the occurrence of fungicide-tolerant pathogens. In addition, chitosan has important biological features, such as biocompatibility, hemostatic, biodegradability, analgesic, antitumor, anticholesterolemic, antioxidative and antimicrobial activities.²⁰ However, the significantly poor solubility of chitosan, caused by the high crystallinity due to the existence of hydrogen bonds and acetamido groups, prevents its wide use. Therefore, it is required to modify the structure of original chitosan to improve its solubility and other properties.

Theoretical calculations have greatly benefited from the development of the density functional theory (DFT) methods. Up to now, there are many calculations arising from DFT, but they have been used mostly within semiempirical methods, Hartree Fock or post-Hartree Fock methods. Recently, however, DFT has enabled theoretical chemistry to predict accurately structures and physical and chemical properties of molecules with theoretical modelling.^{26,27} Considering this, more attention should be paid to the reactivity descriptors as determined directly from DFT calculations. The development of electronic structure methods may provide an insight into the properties of polysaccharides, which was not accessible in older works on this subject.

The present work shows for the first time how the main features of cellulose and chitosan can be predicted using the density functional theory. The theoretical approach can be seen as a first-order approximation, which can be further improved. The theoretical calculations of polysaccharides provide basic knowledge of their structure, properties, and interactions with the environment. Here, we point out its main features with emphasis on the nature of cellulose and chitosan. To the best of our knowledge, no theoretical DFT calculations based on charge distribution, chemical reactivity and electronic properties of the cellulose and chitosan have been reported so far. This encouraged us to study these aspects in detail focusing on cellulose and chitosan. The

purpose of this work is to take a closer look at cellulose and chitosan. Their characterization can provide great opportunities for natural polymer science by using DFT methods. Natural polymers have attracted great interest in the both industrial and academic fields. The calculated data are greatly important as they provide an insight into molecular analysis and can be employed in technological applications.

EXPERIMENTAL

Computational methods

The molecular structures (in dimer forms) of cellulose and chitosan in ground state were optimized by the density functional theory (B3LYP) method with the 6-31G (d, p) basis sets, using Gaussian 09 package program²⁸ and Gaussview molecular visualization program.²⁹ The other calculations were performed by using the hybrid functional and Becke's three parameter functional (B3),³⁰ combined with gradient-corrected correlational functional of Lee, Yang and Parr (LYP),^{31,32} supplemented with standard 6-31G (d, p) basis set.

RESULTS AND DISCUSSION

Molecular geometry of cellulose and chitosan

Geometry optimization of cellulose and chitosan (in dimer forms) were carried out in DFT using the B3LYP/6-31G (d, p) basis set. The optimized structures of cellulose and chitosan are shown in Figure 1 (a, b) as tube (top) and ball&bond type (bottom), respectively. The optimized parameters, such as bond lengths and bond angles, are given in Table 1 in accordance with the atom numbering scheme shown in Figure 1. In the dimer forms of cellulose and chitosan, the C1-C5 bond distance shows values of 1.531 and 1.544 Å, the C4-C5 bond distance shows values of 1.546 and 1.537 Å, the C3-C4 bond distance shows values of 1.546 and 1.537 Å, the C15-O25 bond distance shows values of 1.427 and 1.426 Å, the C19-O26 bond distance shows values of 1.425 and 1.421 Å, the C2-O11 bond distance shows values of 1.396 and 1.405 Å, the C2-O12 bond distance shows values of 1.424 and 1.411 Å, respectively. In cellulose, O42-H43 and O44-H45 bond distances show values of 0.970 and 0.966, respectively. In chitosan, the N42-H43, N42-H44, N45-H46 and N45-H47 bond distances show values of 1.0173, 1.0152, 1.0186 and 1.0176 Å, respectively. In comparison with bond lengths, the N-H bond lengths are calculated as about 1.015, and are slightly longer than the O-H bond lengths of about 0.970 and 0.966. These differences are attributed to the

electronegativity of oxygen (O) and nitrogen (N) atoms. In cellulose, one of the largest bond angles is calculated as 114.231° and attributed to C2–O11–C15, while one of the smallest bond angles is calculated as 104.134° and attributed to C4–O13–H14. In chitosan, one of the largest bond angles is calculated as 115.940° and attributed to C2–O11–C15, while one of the smallest bond angles is calculated as 105.083° and attributed to

O12–C1–C33. The bond angle, in which both cellulose and chitosan connecting two units are calculated as 114.231° and 115.940° , is attributed to C2–O11–C15. Comparing these bond angles, the C2–O11–C15 bond angle of cellulose is smaller than the C2–O11–C15 bond angle of chitosan.

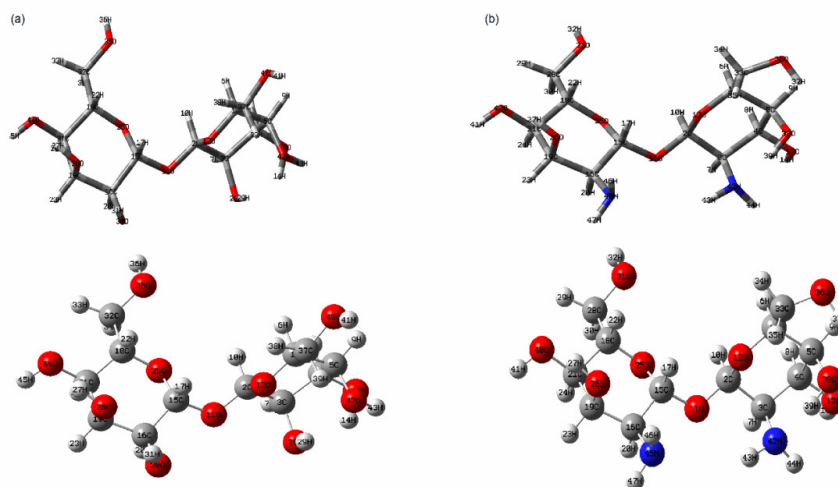


Figure 1: Optimized structure for dimer forms of cellulose (a) and chitosan (b) as tube (top) and ball&bond type (bottom)

Table 1
Optimized structural parameters, such as bond lengths (Å) and bond angles ($^\circ$), for dimer forms of cellulose and chitosan calculated by DFT method using 6-31G (d, p) basis set

DFT/B3LYP			
Parameter	Cellulose	Parameter	Chitosan
<i>Bond length (Å)</i>			
(C1–C5)	1.5311	(C1–C5)	1.5442
(C1–H6)	1.1032	(C1–H6)	1.1033
(C1–O12)	1.4282	(C1–O12)	1.4347
(C1–C37)	1.5245	(C1–C33)	1.5424
(C2–C3)	1.5289	(C2–C3)	1.5332
(C2–C10)	1.1028	(C2–H10)	1.1025
(C2–O11)	1.3963	(C2–O11)	1.4055
(C2–O12)	1.4249	(C2–O12)	1.4114
(C3–C4)	1.5461	(C3–C4)	1.5379
(C3–H7)	1.0948	(C3–H7)	1.1047
(C3–O28)	1.4221	(C3–N42)	1.4683
(C4–C5)	1.5464	(C4–C5)	1.5377
(C4–H8)	1.0977	(C4–H8)	1.1027
(C4–O13)	1.4243	(C4–O13)	1.4239

(C5-H9)	1.0983	(C5-H9)	1.0947
(C5-O42)	1.4293	(C5-O38)	1.418
(O11-C15)	1.3983	(O11-C15)	1.3975
(O13-H14)	0.9742	(O13-H14)	0.9666
(C15-C16)	1.5347	(C15-C16)	1.5345
(C15-H17)	1.0996	(C15-H17)	1.0977
(C15-O25)	1.4275	(C15-O25)	1.4267
(C16-C19)	1.5373	(C16-C19)	1.5449
(C16-H20)	1.0956	(C16-H20)	1.0967
(C16-O30)	1.4106	(C16-N45)	1.46
(C18-C21)	1.5347	(C18-C21)	1.5348
(C18-H22)	1.1001	(C18-H22)	1.1
(C18-O25)	1.4235	(C18-O25)	1.4228
(C18-C32)	1.518	(C18-C28)	1.5185
(C19-C21)	1.5387	(C19-C21)	1.5409
(C19-H23)	1.1031	(C19-H23)	1.1064
(C19-O26)	1.4259	(C19-O26)	1.4216
(C21-H24)	1.0992	(C21-H24)	1.0995
(C21-O44)	1.4353	(C21-O40)	1.4358
(O26-H27)	0.9703	(O26-H27)	0.9707
(O28-H29)	0.9736	(C28-H29)	1.0992
(O30-H31)	0.9693	(C28-H30)	1.1019
(C32-H33)	1.0992	(C28-O31)	1.4199
(C32-H34)	1.1014	(O31-H32)	0.9651
(C32-O35)	1.4204	(C33-H34)	1.0938
(O35-H36)	0.9651	(C33-H35)	1.0975
(C37-H38)	1.0995	(C33-O36)	1.4152
(C37-H39)	1.0958	(O36-H37)	0.9707
(C37-O40)	1.4237	(O38-H39)	0.9839
(O40-H41)	0.9641	(O40-H41)	0.9667
(O42-H43)	0.97	(N42-H43)	1.0173
(O44-H45)	0.9666	(N42-H44)	1.0152
		(N45-H46)	1.0186
		(N45-H47)	1.0176

Bond Angles (°)

(C5-C1-H6)	107.7765	(C5-C1-H6)	108.6524
(C5-C1-O12)	110.7203	(C5-C1-O12)	111.4356
(C5-C1-C37)	113.3641	(C5-C1-C33)	111.3058
(H6-C1-O12)	109.8856	(H6-C1-O12)	109.4919
(H6-C1-C37)	108.2896	(H6-C1-C33)	110.8464
(O12-C1-C37)	106.7633	(O12-C1-C33)	105.0834
(C3-C2-C10)	109.7959	(C3-C2-H10)	110.4025
(C3-C2-O11)	109.0985	(C3-C2-O11)	106.5486
(C3-C2-O12)	109.9077	(C3-C2-O12)	111.0496
(C10-C2-O11)	110.5129	(H10-C2-O11)	110.2508
(C10-C2-O12)	109.1179	(H10-C2-O12)	109.7546
(O11-C2-O12)	108.3887	(O11-C2-O12)	108.7768
(C2-C3-C4)	109.8093	(C2-C3-C4)	108.1943
(C2-C3-H7)	109.0569	(C2-C3-H7)	107.0191
(C2-C3-O28)	112.6821	(C2-C3-N42)	109.4569
(C4-C3-H7)	109.9599	(C4-C3-H7)	109.5061
(C4-C3-O28)	109.1742	(C4-C3-N42)	109.4226
(H7-C3-O28)	106.0823	(H7-C3-N42)	113.1078
(C3-C4-C5)	111.2945	(C3-C4-C5)	110.3345
(C3-C4-H8)	109.7281	(C3-C4-H8)	108.1023
(C3-C4-O13)	109.0902	(C3-C4-O13)	111.5695
(C5-C4-H8)	109.0338	(C5-C4-H8)	107.2326

(C5-C4-O13)	109.253	(C5-C4-O13)	108.9826
(H8-C4-O13)	108.3895	(H8-C4-O13)	110.5263
(C1-C5-C4)	110.9983	(C1-C5-C4)	109.2979
(C1-C5-H9)	108.3349	(C1-C5-H9)	107.875
(C1-C5-O42)	108.3919	(C1-C5-O38)	111.1101
(C4-C5-H9)	109.7391	(C4-C5-H9)	108.6161
(C4-C5-O42)	109.2693	(C4-C5-O38)	113.0004
(H9-C5-O42)	110.0888	(H9-C5-O38)	106.7589
(C2-O11-C15)	114.231	(C2-O11-C15)	115.9407
(C1-O12-C2)	111.687	(C1-O12-C2)	113.7978
(C4-O13-H14)	104.1343	(C4-O13-H14)	107.4379
(O11-C15-C16)	108.5566	(O11-C15-C16)	108.4357
(O11-C15-H17)	110.946	(O11-C15-H17)	110.7181
(O11-C15-O25)	107.2427	(O11-C15-O25)	107.3068
(C16-C15-H17)	110.9345	(C16-C15-H17)	111.2507
(C16-C15-O25)	109.2971	(C16-C15-O25)	109.4734
(H17-C15-O25)	109.7738	(H17-C15-O25)	109.5628
(C15-C16-C19)	109.4395	(C15-C16-C19)	108.6746
(C15-C16-H20)	106.7699	(C15-C16-H20)	106.04
(C15-C16-O30)	113.0835	(C15-C16-N45)	110.8829
(C19-C16-H20)	109.8369	(C19-C16-H20)	108.6236
(C19-C16-O30)	110.3446	(C19-C16-N45)	113.7797
(H20-C16-O30)	107.2547	(H20-C16-N45)	108.5311
(C21-C18-H22)	108.919	(C21-C18-H22)	108.9535
(C21-C18-O25)	107.574	(C21-C18-O25)	107.7149
(C21-C18-C32)	113.0913	(C21-C18-C28)	112.8103
(H22-C18-O25)	110.6433	(H22-C18-O25)	110.6051
(H22-C18-C32)	108.4535	(H22-C18-C28)	108.526
(O25-C18-C32)	108.1667	(O25-C18-C28)	108.2369
(C16-C19-C21)	113.6265	(C16-C19-C21)	113.2218
(C16-C19-H23)	108.5538	(C16-C19-H23)	108.4771
(C16-C19-O26)	106.1715	(C16-C19-O26)	107.419
(C21-C19-H23)	109.3645	(C21-C19-H23)	108.528
(C21-C19-O26)	109.2515	(C21-C19-O26)	109.28
(H23-C19-O26)	109.7953	(H23-C19-O26)	109.8852
(C18-C21-C19)	110.2927	(C18-C21-C19)	110.3863
(C18-C21-H24)	108.5975	(C18-C21-H24)	108.5575
(C18-C21-O44)	108.2449	(C18-C21-O40)	108.0904
(C19-C21-H24)	109.7059	(C19-C21-H24)	109.6672
(C19-C21-O44)	109.0184	(C19-C21-O40)	109.2727
(H24-C21-O44)	110.9676	(H24-C21-O40)	110.8505
(C15-O25-C18)	113.4763	(C15-O25-C18)	113.3265
(C19-O26-H27)	105.9655	(C19-O26-H27)	105.7112
(C3-O28-H29)	105.8951	(C18-C28-H29)	108.0491
(C16-O30-H31)	106.1343	(C18-C28-H30)	108.4138
(C18-C32-H33)	108.1294	(C18-C28-O31)	108.202
(C18-C32-H34)	108.4713	(H29-C28-H30)	108.4143
(C18-C32-O35)	108.0012	(H29-C28-O31)	111.9417
(H33-C32-H34)	108.4645	(H30-C28-O31)	111.6985
(H33-C32-O35)	111.9341	(C28-O31-H32)	107.9034
(H34-C32-O35)	111.7229	(C1-C33-H34)	109.9967
(C32-O35-H36)	107.9461	(C1-C33-H35)	106.7839
(C1-C37-H38)	108.3673	(C1-C33-O36)	112.8635
(C1-C37-H39)	108.7204	(H34-C33-H35)	107.9157
(C1-C37-O40)	107.201	(H34-C33-O36)	107.3033
(H38-C37-H39)	108.5581	(H35-C33-O36)	111.8879
(H38-C37-O40)	111.7285	(C33-O36-H37)	104.7172
(H39-C37-O40)	112.1542	(C5-O38-H39)	104.7633
(C37-O40-H41)	108.0166	(C21-O40-H41)	108.2069

(C5–O42–H43)	104.3755	(C3–N42–H43)	109.5787
(C21–O44–H45)	108.2288	(C3–N42–H44)	109.6562
		(H43–N42–H44)	109.4961
		(C16–N45–H46)	108.4663
		(C16–N45–H47)	109.5326
		(H46–N45–H47)	106.0912

Frontier molecular orbitals of cellulose and chitosan

Frontier molecular orbitals (FMOs), which are the highest occupied molecular orbital (HOMO) and the lowest unoccupied molecular orbital (LUMO), generally play a part in chemical reactions, electrical and optical features.³³ Besides, their energy gap (E_g) has been used to prove the bioactivity from intramolecular charge transfer in recent years.³⁴ The plots of HOMO-1, HOMO and LUMO, LUMO+1 are shown in Figure 2. HOMO shows the ability to donate an electron, while LUMO, as an electron acceptor, shows the ability to obtain an electron. The total energy, dipole moment (μ), HOMO-1, HOMO and LUMO, LUMO+1 energies, energy gap ($E(g)$), electron affinity (A), electronegativity (χ), ionization potential (I), chemical potential (μ_0), hardness (η), global electrophilicity (ω) and global softness (ζ) for the cellulose and chitosan have been calculated at B3LYP/6-31G (d, p) basis set and the results are given in Table 2.

The energy gaps ($E(g)$), electron affinity (A), ionization potential (I), electronegativity (χ), chemical potential (μ_0), hardness (η), global electrophilicity (ω) and global softness (ζ) can be defined as:^{35,36}

$$E(g) = E_{LUMO} - E_{HOMO}, A = -E_{LUMO}, I = -E_{HOMO}, \eta = \frac{I-A}{2}, \mu_0 = \frac{-(I+A)}{2}, \chi = \frac{I+A}{2}, \zeta = \frac{1}{\eta}, \omega = \frac{\mu_0^2}{2\eta}$$

A molecule having a small frontier orbital gap is more polarizable and is generally associated with low kinetic stability and high chemical reactivity.³⁷ The chemical potential, global hardness and electrophilicity will help in many ways to understand the structure of the molecules and their reactivity, with the aid of DFT based descriptors. In cellulose and chitosan, the value of the energy between the HOMO and LUMO is 7.73 and 7.45 eV, respectively, demonstrating that charge transfer occurs much more within chitosan. As shown in Table 2, the chemical potential is negative and it means that cellulose and chitosan are stable.

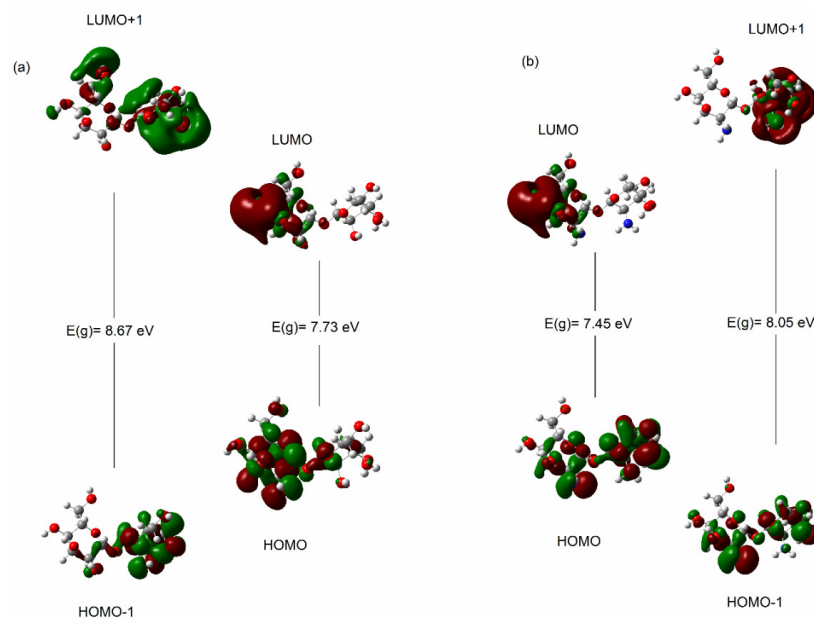


Figure 2: Molecular orbitals (MOs) for dimer forms of cellulose (a) and chitosan (b)

Table 2
Some parameters for dimer forms of cellulose and chitosan calculated by DFT method using 6-31G (d, p) basis set

DFT/B3LYP		
Parameters (eV)	Cellulose	Chitosan
E_{HOMO}	-6.66	-6.35
E_{LUMO}	1.06	1.10
Energy gap 1 [$E(g) = E_{\text{LUMO}} - E_{\text{HOMO}}$]	7.73	7.45
$E_{\text{HOMO}-1}$	-6.86	-6.39
$E_{\text{LUMO}+1}$	1.81	1.65
Energy gap 2 [$E(g) = E_{\text{LUMO}+1} - E_{\text{HOMO}-1}$]	8.67	8.05
SCF energy	35318.71	3423.76
Dipole moment (μ)	5.1184 Debye	9.3157
Ionization energy (I)	6.66	6.35
Electron affinity (A)	-1.06	-1.10
Electronegativity(χ)	2.80	2.62
Chemical potential (μ_0)	-2.80	-2.62
Hardness (η)	3.86	3.72
Global softness (ζ)	0.12	0.13
Global electrophilicity (ω)	1.01	0.92

Mulliken charge analysis of cellulose and chitosan

Mulliken atomic charge calculation has an important role in the application of quantum chemical calculation to a molecular system due to the electronic structure, dipole moment, atomic charge effect, molecular polarizability, and many more properties of molecular systems. These charges are expected to affect the properties, such as electronic parameters, refractivity, dipole moment and polarizability.³⁸ Mulliken atomic charges of cellulose and chitosan (in dimer forms) obtained by using the B3LYP/6-31G (d, p)

method are shown in Figure 3 and listed in Table 3.

As shown in Table 3, the positive charges are localized on the carbon and hydrogen atoms, while negative charges are localized on the oxygen and nitrogen atoms. However, the analysis shows that the presence of the nitrogen atom (N42) creates a negative charge on C3 (about $-0.009e$). In cellulose, the atom O13 shows the largest electronegativity ($-0.570e$) and C15 shows the largest electropositivity ($0.4276e$). In chitosan, the atom N42 shows the largest electronegativity ($-0.625e$) and C2 shows the largest electropositivity ($0.45518e$).

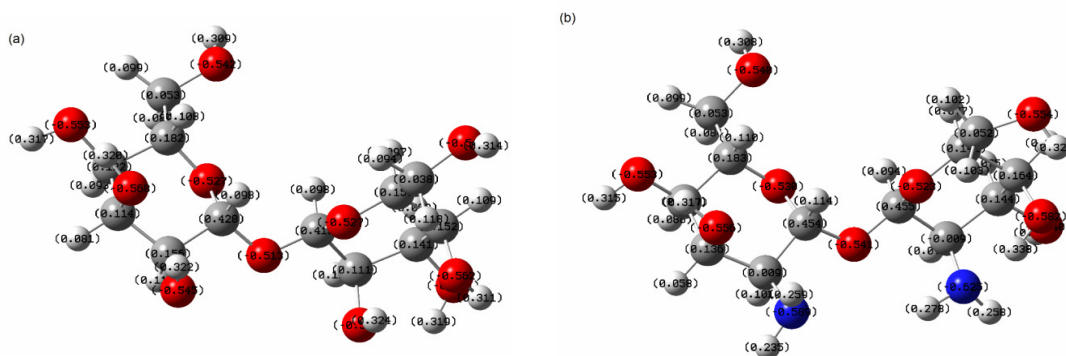


Figure 3: Mulliken atomic charge distributions in dimer forms of cellulose (a) and chitosan (b)

Table 3
Mulliken charges for dimer forms of cellulose and chitosan calculated by DFT method
using 6-31G (d, p) basis set

DFT/B3LYP					
Atom		Cellulose	Atom		Chitosan
1	C	0.15908	1	C	0.14388
2	C	0.41478	2	C	0.45518
3	C	0.11147	3	C	-0.00865
4	C	0.14146	4	C	0.14374
5	C	0.15186	5	C	0.16427
6	H	0.09679	6	H	0.0768
7	H	0.11712	7	H	0.07566
8	H	0.09233	8	H	0.07541
9	H	0.10886	9	H	0.10872
10	H	0.09787	10	H	0.09438
11	O	-0.51306	11	O	-0.54051
12	O	-0.52708	12	O	-0.52314
13	O	-0.57059	13	O	-0.53997
14	H	0.31862	14	H	0.3021
15	C	0.4276	15	C	0.45373
16	C	0.15616	16	C	0.00914
17	H	0.09819	17	H	0.11432
18	C	0.18209	18	C	0.18328
19	C	0.11377	19	C	0.13609
20	H	0.11005	20	H	0.10116
21	C	0.12169	21	C	0.11922
22	H	0.10822	22	H	0.11
23	H	0.08106	23	H	0.058
24	H	0.09328	24	H	0.08809
25	O	-0.52657	25	O	-0.53033
26	O	-0.56826	26	O	-0.55616
27	H	0.32009	27	H	0.31709
28	O	-0.5553	28	C	0.05328
29	H	0.32438	29	H	0.09907
30	O	-0.54546	30	H	0.08378
31	H	0.32157	31	O	-0.53994
32	C	0.05285	32	H	0.30794
33	H	0.09924	33	C	0.05228
34	H	0.08722	34	H	0.10237
35	O	-0.54155	35	H	0.10348
36	H	0.30887	36	O	-0.55419
37	C	0.0379	37	H	0.32649
38	H	0.09427	38	O	-0.58161
39	H	0.11774	39	H	0.33789
40	O	-0.54592	40	O	-0.55315
41	H	0.31391	41	H	0.31537
42	O	-0.56155	42	N	-0.6252
43	H	0.31148	43	H	0.27777
44	O	-0.55348	44	H	0.25776
45	H	0.31695	45	N	-0.58905
			46	H	0.2594
			47	H	0.23475

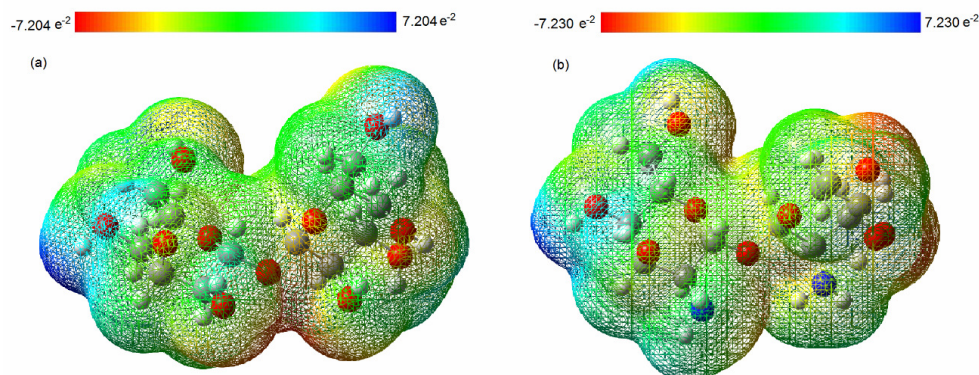


Figure 4: Molecular electrostatic potential surfaces for dimer forms of cellulose (a) and chitosan (b)

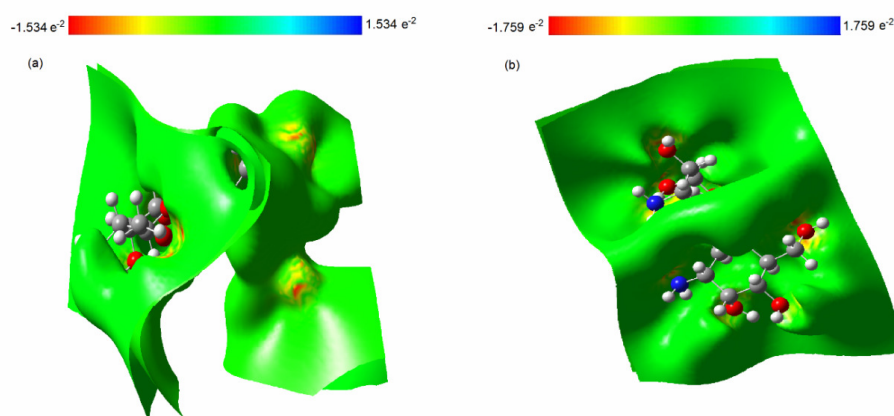


Figure 5: Electrostatic potential surfaces for dimer forms of cellulose (a) and chitosan (b)

Therefore, it can be concluded that not only nucleophilic, but also electrophilic substitution reactions can occur in cellulose and chitosan.

Electrostatic potential and molecular electrostatic potential of cellulose and chitosan

Molecular electrostatic potential (MEP) is related to the electron density and is a very useful descriptor in understanding sites for hydrogen bonding interactions, nucleophilic and electrophilic reactions.^{39,40} Molecular electrostatic potential surfaces were calculated by using the B3LYP/6-31G (d, p) basis set to predict reactive sites of nucleophilic and electrophilic attacks for cellulose and chitosan. Molecular electrostatic potential surfaces of cellulose and chitosan (in dimer forms) are shown in Figure 4. The different values of the electrostatic potential at the surface are shown by different colors. Potential increases in the order red < orange < yellow < green < blue. The negative regions of MEP, which are related to electrophilic reactivity, are seen as red and yellow colors, the positive regions that are related to

nucleophilic reactivity are seen as blue color. From the molecular electrostatic potential surfaces, it is evident that the negative charge covers much more the hydroxyl groups rather than the amine groups, while the positive charge covers the hydroxyl groups. More electronegativity in the hydroxyl groups makes them the most reactive part in cellulose and chitosan. That is, the hydroxyl groups of cellulose and chitosan are reactive sites for both nucleophilic and electrophilic attacks.

The electrostatic potential surfaces of cellulose and chitosan (in dimer forms) are shown in Figure 5. The electrostatic potential (ESP) is related to partial charges and electronegativity. As can be seen from the ESP, the negative ESP is localized more over the oxygen atom and nitrogen and is seen as a reddish blob, while the positive ESP is localized on the rest of the molecules.

CONCLUSION

In the present work, molecular structural parameters, such as bond lengths and bond angles,

and Mulliken atomic charges of cellulose and chitosan (in dimer forms) were investigated by using the density functional theory (DFT/B3LYP) methods with the 6–31G (d, p) basis set. From the optimized geometrical parameters, it is evident that the pyran rings in the disordered molecules are in a slightly distorted chair. Frontier molecular orbitals (FMOs) analysis was used to determine the charge transfer within cellulose and chitosan and their energies showed the chemical activity of cellulose and chitosan. Besides, the electrostatic potential (ESP) and molecular electrostatic potential (MEP) of cellulose and chitosan were investigated by using the same method. From the MEP, it is evident that the positive and negative regions are mainly localized over the –OH groups in cellulose and chitosan. We hope that this study will be useful to those who are in quest of theoretical and experimental evidence for cellulose and chitosan for various materials and applications.

ACKNOWLEDGEMENTS: The author wishes to thank Bitlis Eren University for support with the Gaussian software.

REFERENCES

- ¹ W. Amass, A. Amass and B. Tighe, *Polym. Int.*, **47**, 89 (1998).
- ² L. Illum, *Pharm. Res.*, **15**, 1326 (1998).
- ³ S. Nishimura, O. Kohgo, K. Kurita and H. Kuzuhara, *Macromolecules*, **24**, 4745 (1991).
- ⁴ M. N. R. Kumar, *React. Funct. Polym.*, **46**, 1 (2000).
- ⁵ R. Smith (Ed.), “Biodegradable Polymers for Industrial Applications”, CRC Press, 2005.
- ⁶ D. Klemm, B. Heublein, H. P. Fink and A. Bohn, *Angew. Chem. Int. Ed.*, **44**, 3358 (2005).
- ⁷ J. Credou and T. Berthelot, *J. Mater. Chem. B*, **2**, 4767 (2014).
- ⁸ Y. Kang, Y. Ahn, S. H. Lee, J. H. Hong, M. K. Ku *et al.*, *Fiber. Polym.*, **14**, 530 (2013).
- ⁹ J. T. Oh, J. H. Hong, Y. Ahn and H. Kim, *Fiber. Polym.*, **13**, 735 (2012).
- ¹⁰ R. J. Moon, A. Martini, J. Nairn, J. Simonsen and J. Youngblood, *Chem. Soc. Rev.*, **40**, 3941 (2011).
- ¹¹ A. C. W. Leung, E. Lam, J. Chong, S. Hrapovic and J. H. T. Luong, *J. Nanoparticle Res.*, **15**, 1 (2013).
- ¹² B. Weng, F. Xu, M. Alcoutlabi, Y. Mao and K. Lozano, *Cellulose*, **22**, 1311 (2015).
- ¹³ P. Hou, X. Cheng, J. Qian, R. Zhang, W. Cao *et al.*, *Cement. Concrete Comp.*, **55**, 26 (2015).
- ¹⁴ M. C. Li, Q. Wu, K. Song, C. F. De Hoop, S. Lee *et al.*, *Ind. Eng. Chem. Res.*, **55**, 133 (2015).
- ¹⁵ B. V. Mohite, R. K. Suryawanshi and S. V. Patil, *Cellulose Chem. Technol.*, **50**, 219 (2016).
- ¹⁶ L. Ochiuz, M. Hortolomei, I. Stoleriu and M. Bercea, *Cellulose Chem. Technol.*, **50**, 569 (2016).
- ¹⁷ O. Petrauskaitė, G. Juodzbaly, P. Viskelis and J. Liesiene, *Cellulose Chem. Technol.*, **50**, 23 (2016).
- ¹⁸ P. A. Sandford, in “Chitin and Chitosan”, edited by G. Skjak-Brack, T. Anthosen, P. Sandford, Elsevier, London, 1989, p. 51.
- ¹⁹ B. Launry, J. L. Doublier and G. Cuverlier, in “Functional Properties of Food Macromolecules”, edited by J. R. Mitchell and D. A. Ledwar, London, Elsevier, Applied Science Publisher, 1986, Chap. 1.
- ²⁰ I. Aranaz, M. Mengibar, R. Harris, I. Panos, B. Miralles *et al.*, *Curr. Chem. Biol.*, **3**, 203 (2009).
- ²¹ P. K. Dutta, J. Dutta and V. S. Tripathi, *J. Sci. Ind. Res. India*, **63**, 20 (2004).
- ²² Z. Zheng, J. Jiang, J. Guo, J. Sun and J. Yang, *Org. Electron.*, **33**, 311 (2016).
- ²³ E. Bobu, R. Nicu, P. Obrocea, E. Ardelean, S. Dunca *et al.*, *Cellulose Chem. Technol.*, **50**, 689 (2016).
- ²⁴ I. Kavianinia, P. G. Plieger, N. J. Cave, G. Gopakumar, M. Dunowska *et al.*, *Int. J. Biol. Macromol.*, **85**, 539 (2016).
- ²⁵ B. R. Dos Santos, F. B. Bacalhau, T. Dos Santos Pereira, C. F. Souza and R. Faez, *Carbohydr. Polym.*, **127**, 340 (2015).
- ²⁶ F. Akman, *Can. J. Phys.*, **94**, 583 (2016).
- ²⁷ F. Akman, *Can. J. Phys.*, **94**, 290 (2016).
- ²⁸ M. J. Frisch, G. W. Trucks, H. B. Schlegel, G. E. Scuseria, M. A. Robb *et al.*, Gaussian, Inc., Wallingford CT, 2010.
- ²⁹ R. Dennington, T. Keith and J. Millam, GaussView, Version 5, Semichem Inc., Shawnee Mission KS, 2010.
- ³⁰ A. D. Becke, *Phys. Rev. A*, **38**, 3098 (1988).
- ³¹ C. Lee, W. Yang and R. G. Parr, *Phys. Rev. B*, **37**, 785 (1988).
- ³² A. D. Becke, *J. Chem. Phys.*, **98**, 5648 (1993).
- ³³ P. Politzer, P. R. Laurence and K. Jayasuriya, *Environ. Health Persp.*, **61**, 191 (1985).
- ³⁴ K. Bahgat and S. Fraihat, *Spectrochim. Acta*, **135**, 1145 (2015).
- ³⁵ R. J. Parr, L. V. Szentpaly and S. Liu, *J. Am. Chem. Soc.*, **121**, 1922 (1999).
- ³⁶ T. A. Koopmans, *Physica*, **1**, 104 (1993).
- ³⁷ I. Fleming, *Frontier Orbital and Organic Chemical Reactions*, John Wiley and Sons, New York, 1976.
- ³⁸ M. Govindarajan, M. Karabacak, V. Udayakumar and S. Periandy, *Spectrochim. Acta*, **88**, 37 (2012).
- ³⁹ E. Scrocco and J. Tomasi, *Adv. Quantum Chem.*, **103**, 115 (1978).
- ⁴⁰ F. J. Luque, J. M. Lopez and M. Orozco, *Theor. Chem. Acc.*, **103**, 343 (2000).